Construction and Building Materials 438 (2024) 137096

Contents lists available at ScienceDirect

Construction and Building Materials

journal homepage: www.elsevier.com/locate/conbuildmat

Properties of low sulfur leached spodumene as supplementary cementitious material in ordinary Portland cement

Julia Woskowski [a,b,*], Andreas Neumann [a,b], Hans Roggendorf [a], Ralf Wehrspohn [a,c], Stefan Stöber [a,b]

[a] Institute for Technologies and Economics of Lithium (ITEL), Leipziger Str. 70, Halle (Saale) 06108, Germany
[b] Mineralogy/Geochemistry, Martin Luther University Halle-Wittenberg, Von-Seckendorff-Platz 4, Halle (Saale) 06120, Germany
[c] Microstructure-based material design group, Martin Luther University Halle-Wittenberg, Heinrich-Damerow-Str. 4, Halle (Saale) 06120, Germany

ARTICLE INFO

Keywords:
Leached Spodumene
SCM
Calorimetry
Waste Management
Pozzolanity

ABSTRACT

In the context of the increasing demand for lithium, the extraction of lithium from spodumene is being pursued. During the processing of spodumene, large quantities of leached spodumene concentrate (LSC) are produced as a by-product. To avoid the deposition of the material, potential reuse of the material within the cement industry is investigated. XRD and XRF analyses show that the LSC consists predominantly of leached spodumene and thus of an Al_2O_3 and SiO_2 containing material. The pozzolanic composition of the material suggests a reusability of the material as supplementary cementitious material (SCM) within the cement industry. To test this approach, the hydration properties of LSC powders in combination with OPC cement are investigated. The chemical and mineralogical composition was determined using X-ray methods, followed by the assessment of the hydration behavior of LSC by puzzolanity testing and calorimeter of the heat flow. The tests show that a low-sulfur LSC (up to 1.8 %) is very reactive for mixtures of up to 20 % and produces high mechanical strengths in combination with an OPC. The influence of different raw material sources and process-related fluctuations on the conversion rate from α to β spodumene is negligible.

1. Introduction

Currently, one of the biggest challenges facing the cement industry is the reduction of its carbon footprint. Cement is by far the most commonly used building material [1].The cement industry is the third-largest energy consumer (about 7 %) and the second-largest direct producer of CO_2 (about 27 %) in industry [2]. In 2022, about $4.1 \cdot 10^{12}$ tonnes of cement were produced worldwide [3]. The cement industry is therefore responsible for approx. $2.1 \cdot 10^{12}$ tonnes of CO_2 emissions [4]. Although China was the largest cement producer in 2019 with 56 %, the EU followed in third place with 4.4 % after India (7.8 %) [5]. The high CO_2 emissions are primarily attributed to two factors. First, the energy-intensive primary clinker production accounts for approximately one-third of the CO_2 emissions [2]. Second, the decomposition reaction ($CaCO_3 \rightarrow CaO + CO_2$) occurring during cement production, is responsible for the remaining two-thirds of the CO_2 emissions [2]. CO_2 savings can therefore be achieved primarily by the type of fuel used in clinker production, CO_2-free Ca sources, and by the reduction of clinker in the end product. One option to reduce CO_2 emissions is to add supplementary cementitious materials (SCM) to the cement clinker. These factors reduce the clinker content and they can function as additives to optimize the properties of the respective cement. Currently, SCMs account for about 14 % of the raw meal blend [6]. In Europe the average proportion of clinker in cement is around 76 %, the aim is to reduce the clinker content to below 70 % by 2050 [6].

In the context of the energy transition, there is currently a growing demand for lithium. Lithium possesses unique properties that make it valuable in various applications, including the glass and ceramic industry [7]. However, its most prominent use is in the field of rechargeable batteries [7]. Approx 60 % of the lithium produced worldwide originates from hard rock, the remaining 40 % is extracted from brines [8]. There are various lithium-bearing minerals such as petalite, lepidolite, and zinnwaldite. One of the most important minerals for industrial use is spodumene ($LiAl[Si_2O_6]$). The production of a lithium compound from spodumene concentrate involves typically the acid-roasting process [7,9]. In this process, the mined α-spodumene is

* Corresponding author at: Institute for Technologies and Economics of Lithium (ITEL), Leipziger Str. 70, Halle (Saale) 06108, Germany.
E-mail address: julia.woskowski@lithiuminstitut.de (J. Woskowski).

https://doi.org/10.1016/j.conbuildmat.2024.137096
Received 12 March 2024; Received in revised form 13 May 2024; Accepted 12 June 2024
Available online 17 June 2024

initially heated to 1100 °C, resulting in a phase transformation of α-spodumene via γ-spodumene to β-spodumene [10]. In contrast to the chemically very stable α-spodumene, γ- and β-spodumene are leachable, with β-spodumene being the most suitable [11]. Acid roasting is carried out at about 250 °C using concentrated sulfuric acid. The solid phase is then separated from the sulfuric acid which contains the through ion-exchange-extracted lithium and further processing steps are carried out [10,12]. At the end of the process, a very pure lithium carbonate or lithium hydroxide is obtained.

Pure spodumene contains about 8 wt% Li_2O therefore, most of the spodumene remains as an industrial by-product (leached spodumene concentrate/-abbrev. LSC). Currently, a significant portion of these by-products (LSC) is being deposited, which can lead to environmental issues on one hand and represent a waste of resources on the other hand [13–15].

LSC consists mainly of aluminosilicates ($HAl[Si_2O_6]$) with varying amounts of sulfate and calcium. Initial studies on the use of this by-product as supplementary cementitious materials (SCM) have been conducted by several authors [13,14,16–18]. In various publications, it has been shown that LSC has only a small proportion of reactive aluminosilicate phases despite the high contents of SiO_2 and Al_2O_3 [17, 19,20]. In all these publications, the LSC has a rather high SO_3 content of more than 6 wt%, a residue from leaching with sulfuric acid. [21] citing other researchers, indicate that the elevated SO_3 content might act as a limiting factor in the utilization of LSC as SCM, as higher proportions could potentially compromise the gypsum content in cement.

In this paper, the properties of an LSC with a very low SO_3 content were investigated. Firstly, the composition of the LSC was determined, secondly, initial tests on the reactivity of the material in combination with a CEM I [22] were carried out.

2. Materials

The present LSC originates from experiments, which were conducted on a pilot plant scale and provided by RockTech Lithium Inc. The spodumene concentrate used for the tests originates from four separate locations, with two samples provided from one location. The moisture content in the samples is approx. 22 wt% and was analyzed using a Halogen Moisture Analyzer Excellence Plus HX204 (Mettler Toledo). The pure density of 2.5 g/cm^3 was determined by MVP-D160-E He-pycnometer – Quantachrome multipycnometer (Quantachrome Instruments). The loss on ignition (LOI) of the previously dried samples is 4–6 wt% after 2 hours of annealing at 1000°C. An overview of the samples and selected characteristic properties is listed in Table 1 The provided data represent an average obtained from three measurements each.

For the experiments carried out in this study, the LSC was dried at 40 °C and ground with a disk mill (agate insert) for 60 s at 700 rpm. A grain size analysis was performed on the untreated and prepared specimens using a laser granulometer Mastersizer 3000 (Malvern-Panalytical). For technical reasons, the > 1 mm fraction of the untreated samples was removed beforehand. The results show that the untreated samples have a D_{50} value between 20 and 40 µm, while the treated samples have a D_{50} value between 7 and 11 µm (Fig. 1). The ordinary portland cement (OPC) used is a CEM I 42.5 R [22] from Schwenk Zement GmbH & Co.

Table 1
Sample overview with information on moisture, loss on ignition, pure density and the D_{50} of the treated samples.

Sample	moisture [wt %]	loss on ignition [wt%]	pure density [wt %]	D_{50} (treated)
1.1 LSC	20.69 ±0.27	4.55 ±0.07	2.49 ±0.01	9.2
1.2 LSC	23.76 ±0.08	5.50 ±0.08	2.46 ±0.01	10.1
2 LSC	23.45 ±0.05	4.52 ±0.03	2.48 ±0.01	10.7
3 LSC	23.06 ± 1.14	4.33 ±0.03	2.54 ±0.01	9.6
4 LSC	20.86 ±1.09	4.66 ±0.26	2.52 ±0.01	8.5

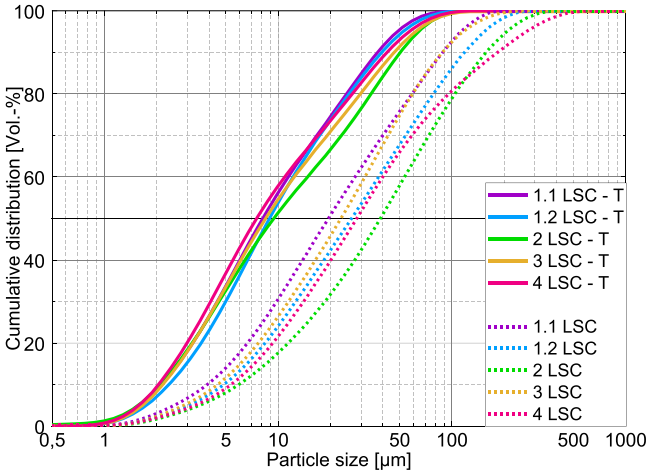

Fig. 1. Grain size distribution of the treated (LSC - T) and untreated LSC samples. After grinding the material, it has an grain size (D_{50}) of 7–11 µm, which corresponds approximately to the grain size of the CEM I 42.5 R used.

3. Methods

3.1. Chemical analysis (XRF and ICP-MS)

The X-ray fluorescence analyses (XRF) were performed using an S8 TIGER 2 (Bruker-AXS). The chemical composition was determined quantitatively with the certified GEO-QUANT-Advanced standard, by applying the Spectra Plus software. Sulfur and Lithium contents were measured separately by ICP-MS at ALS-Global in Ireland.

3.2. XRD/Rietveld

The phase compositions of the LSC samples were determined by Theta/Theta X-ray diffractometer X'Pert Powder (Malvern-Panalytical) featuring a Cu tube ($\lambda_{K\alpha}$=1.5406 Å) operated at a current of 40 mA and a voltage of 45 kV. The counting time per step was 178.245 s and a Pixcel Line detector was used. For the identification of the starting materials, the databases ICDD Version 2004 and COD 2016 were utilized. Rietveld refinements [23] were performed using TOPAS-Academic V7 [24] software. The CIF files were retrieved from the ICSD database 2023/2 and are listed in Table 2.

The quantification of the crystalline and amorphous fractions was determined by the Rietveld method (XRD) using 10 wt% rutile (TiO_2) as an internal standard. The R_{wp} value (residual value/quality factor) of the performed Rietveld refinements was below 6 for all samples [25].

3.3. Scanning electron microscopy/ energy dispersive X-ray spectroscopy – SEM/EDS

Samples 1.2 LSC and 3. LSC were examined with SEM. The studies

Table 2
Overview of the CIF files used for Rietveld refinement from the ICSD, the chemical formula, and the name used in this report.

ICSD-number	chemical composition	mineral mame/compound
9161	TiO_2	Rutile
9668	$LiAl[Si_2O_6]$	α -Spodumene
69394	$LiAl[Si_2O_6]$	β -Spodumene
24897	$LiAl[Si_2O_6]$	γ -Spodumene
67212	$HAl[Si_2O_6]$	leached α -Spodumene
69215	$HAl[Si_2O_6]$	leached β -Spodumene
16331	SiO_2	Quartz
92567	$Ca[SO_4]$ x 2 H_2O	Gypsum
22022/654	$(Ca, Na)[(Al,Si)_4O_8]$	Anorthite
9770	$Na[AlSi_3O_8]$	Albite

were performed using a Tescan CLARA equipped with an Ultim Max S100 EDX detector (Oxford Instruments). The previously unground but dried samples were attached to a carbon tape and coated with carbon.

3.4. Pozzolanicity/Frattini method

To test the pozzolanicity of the samples, the Frattini test according to DIN EN 196–5 [26] was carried out after 8 and 15 days. In this regard, the LSC samples, along with a reference sample of α-spodumene (10 wt %), were mixed with a CEM I 42.5 R cement. Cement blends with 10, 15, and 20 wt% LSC additives were tested.

3.5. Heat flow calorimetry

For the determination of the heat of hydration, 5.0 g composed of CEM I 42,5 R and LSC (10 % and 20 %) were prepared with a water/binder weight ratio of 0.5. The heat of hydration was investigated with an isothermal calorimeter TAM-Air (TA Instruments). The heat flow was recorded for 160 hours. Measurements were carried out by SCHWENK Zement GmbH & Co. KG. The results are shown in Fig. 4.

3.6. TG-DSC/MS

The thermogravimetry and differential scanning calorimetry (TG-DSC) (NETZSCH STA 449 F3 Jupiter®) with coupled mass spectrometry (MS) (QMS 403 D Aeolos) analysis was performed. The samples were heated under Argon-atmosphere from room temperature to 1100 °C at a heating rate of 10 °K/min using a covered corundum crucible. The program Proteus version 6 was used to evaluate the TG-DSC data. The MS data was analyzed with the program Aeolus.

3.7. Mechanical properties

The tests of the compressive strength were carried out following the standard DIN EN 196–1 [27]. A testing device from Strassentest Baustoff-Prüfsystheme was used. A CEM I 42.5 R was applied to produce the test specimens. In addition to a reference sample made of pure CEM I as a binder for comparison purposes, binder blends of CEM I with additions of 10, 15, and 20 % LSC were tested. An overview of the blends can be seen in Table 3 Following the requirements of DIN EN 196–1 [27]. The results of the compressive strength are based on 6 measurements.

4. Results and discussion

4.1. Chemical analysis (XRF and ICP-MS)

The chemical composition of the LSC, shown in Table 4, indicates that the material consists of approx. 90 wt% SiO_2 and Al_2O_3. In addition, the chemical concentrations of Fe_2O_3, CaO, K_2O, MgO, and SO_3 were determined in all samples. The overall composition corresponds to the composition of residues from spodumene lithium production, as described in other publications [13,14,17,18]. As sulfur and calcium are introduced to the material by the leaching process, their concentration in the material depends on the specific process steps and can vary in different publications. The results of the XRF and ICP-MS analysis do not show any contents that are critical for the application of this material as SCM. A slightly increased sulfur content in sample 1.2 LSC and an increased amount of residual lithium in samples 1.2 LSC and 3 LSC are noticeable and might be due to incomplete leaching or phase conversion. Sample 1.2 LSC also showed an increased LOI of 5.5 wt%.

Table 3
Composition of the test specimens for compressive strength and bending tensile strength testing according to DIN EN 196–1 [27].

LSC [%]	LSC [g]	CEM I 42,5 R [g]	Sand [g]	Water [g]	Sum [g]
0	-	450	1350	225	2025
10	45	405	1350	225	2025
15	67,5	382,5	1350	225	2025
20	90	360	1350	225	2025

4.2. XRD/Rietveld-LSC

The XRD (Fig. 2, Table 5, as well as the supplementary information Fig. S1-S4) analyses showed that most LSC samples contain primarily the different modifications of leached and pristine spodumene. The leached modifications of the γ- and β-spodumene account for approx. 65 wt% in the samples. The proportion of residual spodumene modifications is much lower (< 10 wt%). In sample 1.2 LSC no pristine spodumene phases could be detected, which indicates almost complete leaching of this sample. In comparison, sample 3 LSC contained a high proportion of residual α -spodumene (8 wt%). Quartz, feldspar, and gypsum occur as minor phases. The calculated amorphous content using the Rietveld method in the samples ranges between 1 and 15 wt%.

Overall, the composition of the samples exhibited considerable variability. Sample 2 LSC has a large amount of leached β-spodumene (58 wt%), whereas sample 1.1 LSC has an amount of only 40 wt%. The presence of α-spodumene in sample 3 LSC, as well as an increased proportion of leached γ-spodumene, as observed in samples 1.1 LSC and 1.2 LSC, suggests that the transformation of α-spodumene to β-spodumene was not completed. The incomplete phase transformation in sample 3 LSC also explains the increased residual lithium content of this sample. Since α-spodumene is not leachable, the lithium remains in the crystal lattice of the α-spodumene. An increased residual lithium content was also found in sample 1.2 LSC, even though no remnants of residual spodumene could be detected in the sample. In addition, this sample contains 1.75 wt% SO_3, which is seven times higher than in other samples (Table 5). This could be an indication that the sample was not washed after sufficient neutralization. This issue indicates that acid roasting as well as the leaching process needs accompanying phase characterizations for quality control.

4.3. TG-DSC/MS

The TG-DSC results of the raw material (LSC) exemplified by samples 1.2 LSC and 3. LSC is shown in Fig. 3. An initial loss of mass up to approximately 100 °C is due to the evaporation of remaining adhesive water. The TG curve shows a distinct mass loss of 3.75 wt% (3 LSC) and 3.91 wt% (1.2 LSC) between 100 and 900 °C. The MS analysis has shown that this is due to the release of OH or H_2O. This observation agrees with those of Müller, et al. [28], who attribute this mass loss to the dehydration of $HAl[Si_2O_6]$ according to the reaction (Eq. 1):

$$HAlSi_2O_6 \rightarrow Al\ Si_2O_{5.5} + 0.5\ H_2O \quad (1)$$

For a pure material ($HAl[Si_2O_6]$), this would stoichiometrically correspond to a mass loss of 4.99 %. Since the material investigated in this study originates from natural resources featuring gangue and which was not completely converted during processing, a lower mass loss as seen here is to be expected. Between 1000 and 1100 °C a prominent exothermic peak can be seen, which is not accompanied by a mass change. A subsequent XRD examination of the material has shown that this is due to mullite formation.

4.4. Microstructure: scanning electron microscopy/ energy dispersive X-ray spectroscopy –

SEM analysis confirmed the phase assemblages found by XRD. In contrast to the other samples, sample 1.2 LSC shows noticeable, needle-shaped gypsum crystals (Fig. 4). In contrast to XRD, this method was able to detect the presence of potassium-containing mica. However, its total content in the sample is presumably so low that potassium-

Table 4
Chemical composition of LSC samples measured by XRF. Sulfur (SO_3) and lithium (Li) were analyzed by ICP-MS, all data in wt%.

	XRF									ICP-MS	
Sample	LOI	SiO_2	Al_2O_3	Fe_2O_3	CaO	K_2O	MgO	Mn_2O_3	Others	SO_3	Li
1.1 LSC	4.6	65.8	25.7	1.2	0.6	0.6	0.6	0.1	0.8	0.25	0.11
1.2 LSC	5.5	65.3	25.1	1.5	1.0	0.7	0.7	0.1	0.1	1.78	0.30
2 LSC	4.5	66.3	24.6	1.3	0.9	0.7	1.1	0.2	0.4	0.28	0.15
3 LSC	4.3	68.3	25.1	0.7	0.2	0.6	0.2	-	0.6	0.23	0.36
4 LSC	4.7	65.4	24.3	1.3	0.9	0.7	1.1	0.3	1.3	0.18	0.18

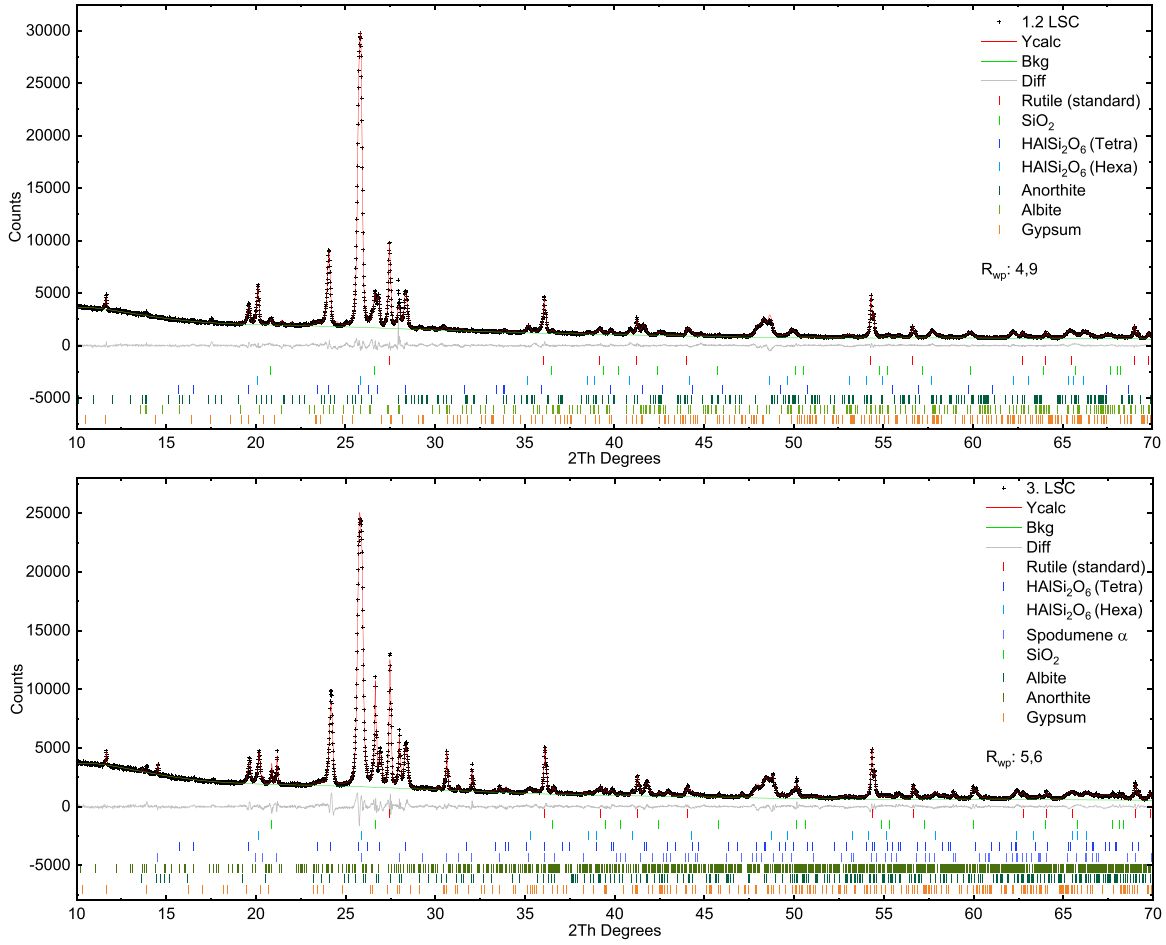

Fig. 2. Rietveld refinement of sample 1.2 LSC and 3.LSC with 10 % Rutile (internal standard). The main phases are the leached β and γ spodumene. Quartz, feldspar, and gypsum were found as minor phases.

Table 5
Rietveld refinement of sample 1.2 LSC with 10 % Rutile (internal standard). The main phases are the leached β and γ spodumene. Quartz and feldspar were found as minor phases.

Phase	1.1 LSC	1.2 LSC	2 LSC	3 LSC	4 LSC
Rutile (internal standard)	10	10	10	10	10
leached γ-spodumene	24	27	6	16	5
leached β-spodumene	41	40	58	44	67
α-Spodumene	-	-	-	8	1
β-Spodumene	-	-	4	-	-
γ-Spodumene	2	-	5	-	3
Quartz	10	4	7	6	6
Gypsum	-	1	-	> 1	-
Feldspar	7	10	10	7	8
Amorphous fraction	15	9	2	8	1

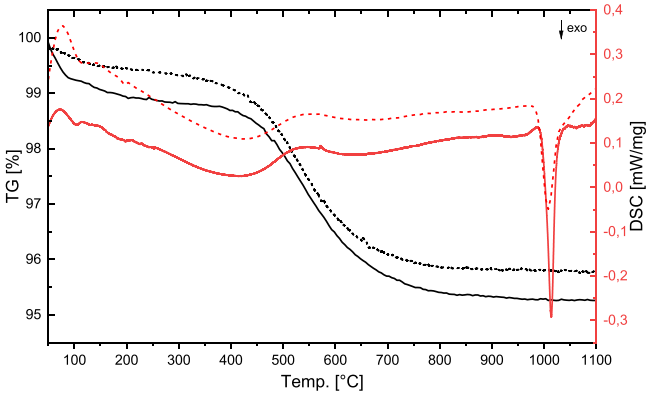

Fig. 3. TG-DSC analysis of the raw material (dashed line 1.2 LSC, solid line 3 LSC) heated up to 1100 °C, heating rate 10° K/min.

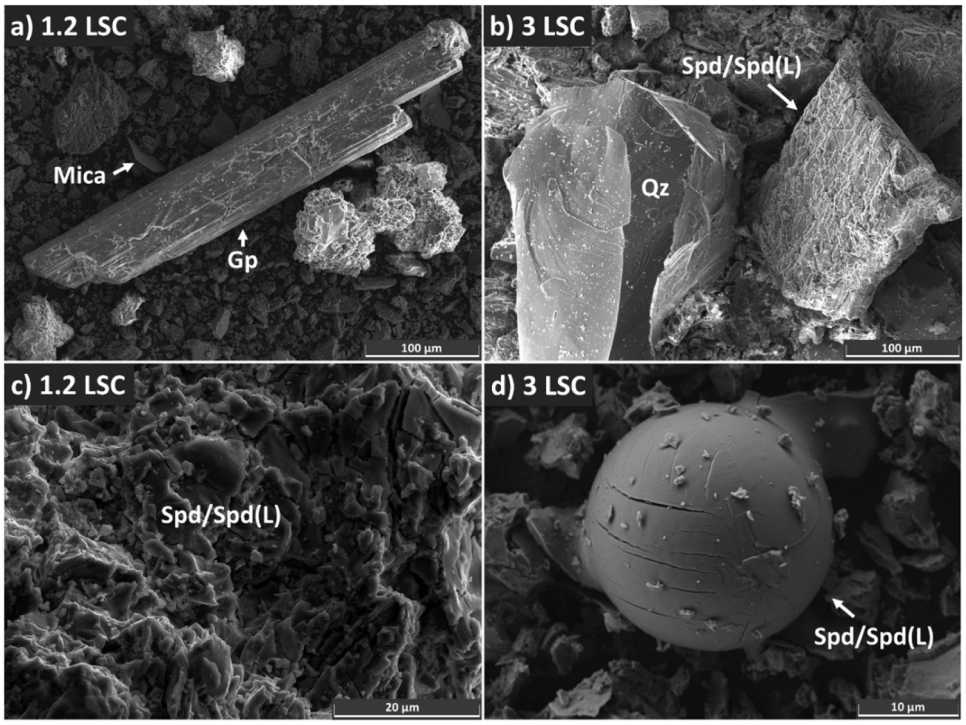

Fig. 4. SEM images of the dried but untreated 1.2 LSC (a and c) and 3 LSC (b and d). The abbreviations used indicate Gypsum (Gp), quartz (Qz), spodumene (Spd), and leached spodumene (Spd(L)).

containing mica was no longer detectable by XRD. Occasionally, spherical particles with a chemical composition similar to spodumene could be determined in sample 3 LSC. These are presumably melting droplets of b-spodumene that formed during the temperature treatment and cooled down again quickly. Fig. 5 and Fig. 6

4.5. Pozzolanicity/Frattini method

The pozzolanic tests show that all tested mixtures of the LSC in combination with a CEM I 42.5 R were in the pozzolanic range after 8 and 15 days (Fig. 3). The lower CaO concentration after 15 days indicates that CSH phases are still being formed. In contrast, the Frattini reference sample with 10 wt% α-spodumene was not pozzolanic after 8 nor after 15 days. This suggests that the crystal lattice of the a-spodumene is too dense, and the Si-Ions are not available for a reaction with the calcium. Hence, a disproportionately high concentration of α-spodumene could potentially impede the reactivity of LSC. However, sample 3 LCS containing 8 wt% α-spodumene does not exhibit diminished reactivity. This suggests that an incomplete phase transformation can be tolerated to some extent without affecting negatively the pozzolanicity of LSC. Furthermore, the distinct difference in terms of different proportions of β-spodumene does not have a noticeable effect on the pozzolanicity either. The performance of sample 1.2 LSC is outstanding. It is located in the pozzolanic field, though the measuring points are noticeably shifted (lower Ca^{2+} concentrations and higher OH^- contents). This is probably due to the increased SO_3/gypsum content in this sample.

Considering the Rietveld quantification results, which indicate amorphous content ranging from 1 % to 15 %, it is evident that pozzolanic activity is not primarily influenced by the amorphous content of

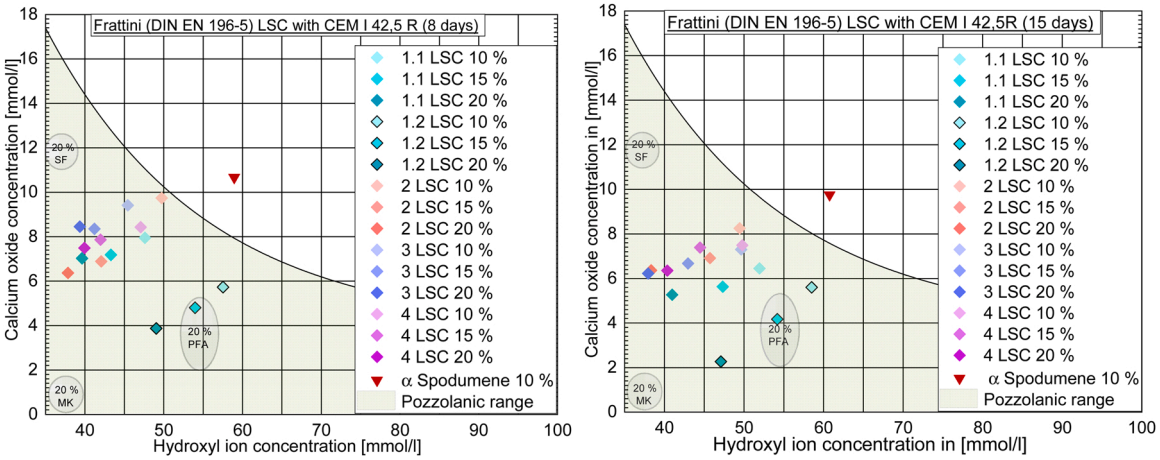

Fig. 5. Pozzolanicity test according to DIN EN 196–5 on different admixtures of LSC samples and α spodumene with a CEM I 42.5 R from Schwenk, results after 8 days (left) and 15 days (right). When the data points lie within the green range, they exhibit pozzolanic properties. For comparison purposes, the pozzolanic ranges of silica fume (SF), metakaolin (MK), and pulverized fly ash (PFA) were given [29–31].

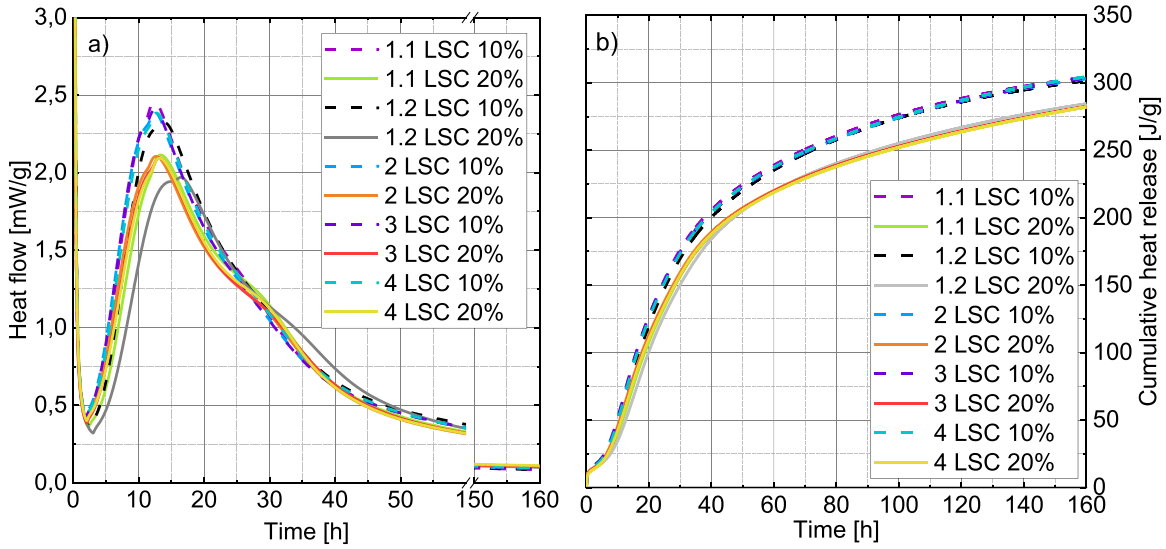

Fig. 6. : Hydration heat of CEM I 42,5 with addition LSC (10 % and 20 %). In figure a) the heat flow is given in [mW/g], in figure b) the cumulative heat release is given in [J/g].

the LSC samples (cf. Table 5). Evidently, the SiO_2 present in the leached γ and β spodumene exhibits a lesser degree of chemical binding, such that its interaction with the cementitious matrix is possible.

4.6. Heat flow calorimetry

The Investigation of the hydration heat showed that an increase in LSC reduces the overall hydration heat. An addition of 10 wt% LSC (dashed lines) showed a heat flow of 300 J/g after 160 hours, while an LSC proportion of 20 wt% (solid lines) showed a heat flow of 260 J/g (Fig. 4b). The main peak, due to the formation of C-S-H phases and portlandite [32], appeared after approx. 12 hours in calorigrams of both blends (Fig. 4a). In addition to the main peak of hydration, a shoulder can be observed after approx. 29 hours on the descending branch of the main peak, which is probably due to the formation of secondary Aluminat-Ferrat- triosulfate (AFt/i.e. Ettringite) [32]. This shoulder is more pronounced in the 20 % mixture. Despite the differences in the composition of the samples, they behave similarly and are reproducible. Sample 1.2 LSC exhibited a slight deviation, the peak maxima were shifted to the right times. The main hydration peak of the 10 wt% blend showed a delay of about 2 hours, while the 20 wt% blend shows a delay of about 3–4 hours. The second hydration peak of the 20 % blend also revealed a more pronounced expression (i.e. the heat flow is increased) of this peak in addition to the time delay.

4.7. Mechanical properties

In order to test the performance of the LSC as SCM, the compressive strength [27] of the samples 1.2 LSC and 3 LSC were tested after 7 and 28 days and compared to the reference sample with pure CEM I. LSC mixtures of 10, 15 and 20 wt% were tested. The test specimens were visually checked and were of flawless quality. The test results are shown in Fig. 7, primary data in the supplementary information (Table. S1). After 7 days, a decrease in compressive strength could be observed with increasing LSC content (1.2 LSC: −15.9 %; −16.4 %; −18,7 %) (3 LSC: −9.1 %; −12.3 %; −17.5 %) compared to the reference sample with pure CEM I. The sample 1.2 LSC consistently exhibits slightly lower strength than sample 3 LSC. This could be due to the higher sulfur content, but it should be noted that the standardization regulation [27] used allows deviations of up to 10 % from the mean value and a repetition of the test is generally recommended. Therefore, without further repetition of this test, it is not possible to say whether this observation is

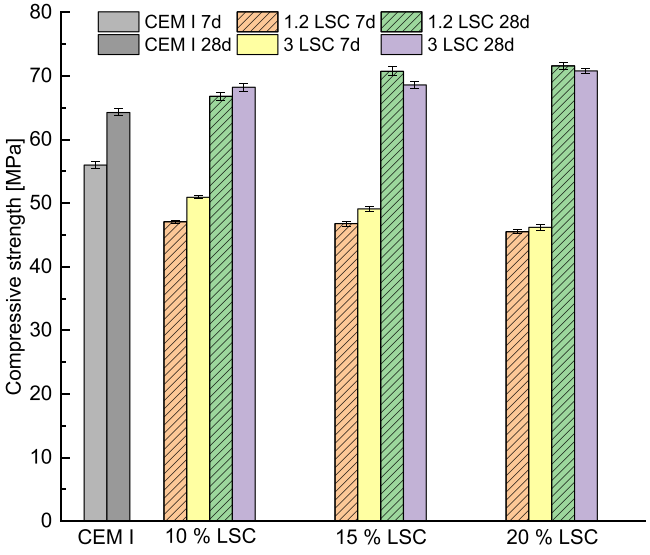

Fig. 7. Results of compressive strength after 7 and 28 days with LSC mixtures of samples 1.2 LSC and 3 LSC of 0, 10, 15 and 20 %. Specify with error bar. The standard error in relation to the mean value is below 0.7 MPa for all measurements.

conclusive. After 28 days, the compressive strength of the test specimens increases noticeably with increasing LSC content (1.2 LSC: 3.9 %; 10.1 %; 11.4 %) (3 LSC: 6.2 %; 6.7 %; 10.2 %). Hence, a significant effect of the sulfur content on the mechanical strength of the samples could not be observed.

5. Conclusions

This study investigates LSC samples with low SO_3 contents derived from the acid-roasting process of Lithium extraction from spodumene. Of particular interest were the chemical composition, qualitative and quantitative phase analysis, as well as an initial examination of the material with regard to its pozzolanic properties. To sum up the results, the following statements can be made:

1. The XRF investigations show that the material consists of about 65 wt% SiO_2 and about 25 wt% Al_2O_3. In addition, other elements such as potassium, calcium, iron, and magnesium occur in significantly lower concentrations. No critical element concentrations were found which would prevent the use of the materials as SCM.
2. ICP measurements show a sulfur content, reported as SO_3, of 0.23–1.75 wt% and a residual lithium (Li) content of 0.11–0.36 wt%.
3. The qualitative and quantitative XRD analysis showed that most of the SiO_2 and Al_2O_3 are bound in the form of $HAl[Si_2O_6]$. In addition, minor amounts of quartz, feldspars, gypsum, and spodumene modifications can be observed. In addition, mica could also be identified as a secondary phase by SEM analysis, although this could not be detected in XRD. The phase composition of the individual samples varies in part extensively.
4. The pozzolanic studies of the LSC showed pozzolanic properties of the material in combination with a CEM I 42.5 R with a LSC content between 10 and 20 wt%. The SO_3 (gypsum) content influences the pozzolanic activity. However, this does not influence the reaction negatively.
5. The calorimetric investigations showed a decrease in the heat of hydration with increasing LSC content. The main hydration peak (maximum heat flow) appears after approx. 12 hours, whereby with increasing LSC a second maximum becomes increasingly apparent after approx. 29 hours. An increased SO_3 content retards slightly the reaction.
6. Tests of the compressive strength show a reduced early strength after 7 days compared to the reference sample and an increased late strength after 28 days. The compressive strength improves with increasing LSC content and is most pronounced with the addition of 20 wt% LSC. The results indicate a slightly more pronounced reduction in early strength after 7 days in the sample 1.2. LSC with increased sulfur content. However, further tests are required to check whether the impact of the given sulfur content is significant.

The results of this study indicate that the LSC investigated is well suited for use as an SCM. The influence of different raw material sources and process-related fluctuations on the conversion rate from α to β spodumene is negligible. Sulfur had the major impact on the properties of the material as SCM. The sulfur contents of up to 1.8 % investigated here did show a negative effect on the strength development of the material.

CRediT authorship contribution statement

Andreas Neumann: Writing – review & editing, Data curation, Conceptualization. **Hans Roggendorf:** Writing – review & editing, Supervision, Project administration. **Julia Woskowski:** Writing – original draft, Visualization, Investigation, Formal analysis, Data curation, Conceptualization. **Ralf Wehrspohn:** Writing – review & editing, Supervision, Project administration. **Stefan Stöber:** Writing – review & editing, Supervision, Conceptualization.

Declaration of Competing Interest

The authors declare the following financial interests/personal relationships which may be considered as potential competing interests: Julia Woskowski reports financial support was provided by Freundeskreis der Deutschen Lithiuminstitues. Andreas Neumann reports financial support was provided by Schwenk Zement GmbH & Co KG, Günter Papenburg ag, RockTech Lithium Inc. Julia Woskowski, Andreas Neumann, Ralf Wehrspohn, has patent #EP24156323 pending to ITEL. If there are other authors, they declare that they have no known competing financial interests or personal relationships that could have appeared to influence the work reported in this paper.

Data availability

Data will be made available on request.

Acknowledgment

The authors gratefully acknowledge the facilities, scientific and technical support of the Mineralogy/Geochemistry division of the Martin-Luther-Universität Halle-Wittenberg. The authors would like to thank RockTech Consulting GmbH, SCHWENK Zement GmbH, Günter Papenburg AG and the Friends of ITEL – Deutsches Lithiuminstitut GmbH of their financial support for this project.

Appendix A. Supporting information

Supplementary data associated with this article can be found in the online version at doi:10.1016/j.conbuildmat.2024.137096.

References

[1] K. Korczak, M. Kochański, T. Skoczkowski, Mitigation options for decarbonization of the non-metallic minerals industry and their impacts on costs, energy consumption and GHG emissions in the EU - systematic literature review, J. Clean. Prod. 358 (2022) 132006, https://doi.org/10.1016/j.jclepro.2022.132006.
[2] IEA - International Energy Agency, Technology Roadmap - Low-Carbon Transition in the Cement Industry (2018).
[3] USGS, Mineral commodity summaries 2023; 2023.
[4] Supriya, R. Chaudhury, U. Sharma, P.C. Thapliyal, L.P. Singh, Low-CO2 emission strategies to achieve net zero target in cement sector, J. Clean. Prod. 417 (2023) 137466, https://doi.org/10.1016/j.jclepro.2023.137466.
[5] Y. Guo, L. Luo, T. Liu, L. Hao, Y. Li, P. Liu, T. Zhu, A review of low-carbon technologies and projects for the global cement industry, J. Environ. Sci. (China) 136 (2024) 682–697, https://doi.org/10.1016/j.jes.2023.01.021.
[6] P. Haslauer, R. Pomberger, T. Nigl, M. Rahnama Mobarakeh, E. Lachner, T. Kienberger, Einflüsse von Kreislaufwirtschaftsmaßnahmen auf Ressourcennutzung und Dekarbonisierung in der Stahl- und Zementindustrie, BHM Berg. - und H. üttenmännische Mon. 168 (2023) 318–324, https://doi.org/10.1007/s00501-023-01366-z.
[7] M. Schmidt, Rohstoffrisikobewertung-Lithium (DERA Rohstoffinformationen 33), Berlin: Deutsche Rohstoffagentur (DERA) in der Bundesanstalt für Geowissenschaften und Rohstoffe (2017).
[8] M. Schmidt, D. Bastian, C. Kresse, Rohstoffrisikobewertung – Lithium (DERA Rohstoffinformationen 54), Berlin: Deutsche Rohstoffagentur (DERA) in der Bundesanstalt für Geowissenschaften und Rohstoffe (2023).
[9] N.K. Salakjani, P. Singh, A.N. Nikoloski, Production of lithium –a literature review. Part 2. Extraction from spodumene, Miner. Process. Extr. Metall. Rev. 42 (2021) 268–283, https://doi.org/10.1080/08827508.2019.1700984.
[10] N.P. Kotsupalo, L.T. Menzheres, A.D. Ryabtsev, V.V. Boldyrev, Mechanical activation of α-spodumene for further processing into lithium compounds, Theor. Found. Chem. Eng. 44 (2010) 503–507, https://doi.org/10.1134/S0040579510040251.
[11] C. Dessemond, G. Soucy, J.-P. Harvey, P. Ouzilleau, Phase Transitions in the α–γ–β Spodumene Thermodynamic System and Impact of γ-Spodumene on the Efficiency of Lithium Extraction by Acid Leaching, Minerals 10 (2020) 519, https://doi.org/10.3390/min10060519.
[12] C. Dessemond, F. Lajoie-Leroux, G. Soucy, N. Laroche, J.-F. Magnan, Revisiting the traditional process of spodumene conversion and impact on lithium extraction. In: Extraction 2018: Proceedings of the First Global Conference on Extractive Metallurgy, 2281–2291; 2018.
[13] H. Tan, X. Li, C. He, B. Ma, Y. Bai, Z. Luo, Utilization of lithium slag as an admixture in blended cements: Physico-mechanical and hydration characteristics, J. Wuhan. Univ. Technol. -Mater. Sci. Ed. 30 (2015) 129–133, https://doi.org/10.1007/s11595-015-1113-x.
[14] T. Zhang, B. Ma, H. Tan, X. Liu, P. Chen, Z. Luo, Effect of TIPA on mechanical properties and hydration properties of cement-lithium slag system, J. Environ. Manag. 276 (2020) 111274, https://doi.org/10.1016/j.jenvman.2020.111274.
[15] Y. He, Q. Zhang, Q. Chen, J. Bian, C. Qi, Q. Kang, Y. Feng, Mechanical and environmental characteristics of cemented paste backfill containing lithium slag-blended binder, Constr. Build. Mater. 271 (2021) 121567, https://doi.org/10.1016/j.conbuildmat.2020.121567.
[16] H. Tan, M. Li, X. He, Y. Su, J. Zhang, H. Pan, J. Yang, Y. Wang, Preparation for micro-lithium slag via wet grinding and its application as accelerator in Portland cement, J. Clean. Prod. 250 (2020) 119528, https://doi.org/10.1016/j.jclepro.2019.119528.
[17] B. Li, R. Cao, N. You, C. Chen, Y. Zhang, Products and properties of steam cured cement mortar containing lithium slag under partial immersion in sulfate solution, Constr. Build. Mater. 220 (2019) 596–606, https://doi.org/10.1016/j.conbuildmat.2019.06.062.

[18] M. Zhai, J. Zhao, D. Wang, Y. Wang, Q. Wang, Hydration properties and kinetic characteristics of blended cement containing lithium slag powder, J. Build. Eng. 39 (2021) 102287, https://doi.org/10.1016/j.jobe.2021.102287.
[19] P. Dong, M.R. Ahmad, B. Chen, M.J. Munir, S.M. Saleem Kazmi, Preparation and study of magnesium ammonium phosphate cement from waste lithium slag, J. Clean. Prod. 316 (2021) 128371, https://doi.org/10.1016/j.jclepro.2021.128371.
[20] Z. Liu, J. Wang, Q. Jiang, G. Cheng, L. Li, Y. Kang, D. Wang, A green route to sustainable alkali-activated materials by heat and chemical activation of lithium slag, J. Clean. Prod. 225 (2019) 1184–1193, https://doi.org/10.1016/j.jclepro.2019.04.018.
[21] Y. He, S. Liu, R.D. Hooton, X. Zhang, S. He, Effects of TEA on rheological property and hydration performance of lithium slag-cement composite binder, Constr. Build. Mater. 318 (2022) 125757, https://doi.org/10.1016/j.conbuildmat.2021.125757.
[22] Beuth-publishing, DIN En, DIN EN 197-1:2004-08, Composition, specifications and conformity criteria for common cements; German version (2004).
[23] H.M. Rietveld, Line profiles of neutron powder-diffraction peaks for structure refinement, Acta Crystallogr. 22 (1967) 151–152, https://doi.org/10.1107/S0365110×67000234.
[24] R.W. Cheary, A. Coelho, A fundamental parameters approach to X-ray line-profile fitting, J. Appl. Crystallogr. 25 (1992) 109–121, https://doi.org/10.1107/S0021889891010804.
[25] B.H. Toby, R factors in rietveld analysis: how good is good enough? Powder Diffr. 21 (2006) 67–70, https://doi.org/10.1154/1.2179804.
[26] Beuth-publishing, DIN En, DIN EN 196-5:1990-03, Methods of testing cement - Part 5: Pozzolanicity test for pozzolanic cement; German version (1990).
[27] Beuth-publishing, DIN En, DIN EN 196-1:2005-05, Methods of testing cement Part 1: Determination of strength;German version EN 196-1:2005-05; German version (2005).
[28] G. Müller, M. Hoffmann, R. Neeff, Hydrogen substitution in lithium-aluminosilicates, J. Mater. Sci. 23 (1988) 1779–1785.
[29] F. Faleschini, K. Toska, M.A. Zanini, F. Andreose, A.G. Settimi, K. Brunelli, C. Pellegrino, Assessment of a municipal solid waste incinerator bottom ash as a candidate pozzolanic material: comparison of test methods, Sustainability 13 (2021) 8998, https://doi.org/10.3390/su13168998.
[30] F. Elyasigorji, F. Farajiani, M. Hajipour Manjili, Q. Lin, S. Elyasigorji, V. Farhangi, H. Tabatabai, Comprehensive review of direct and indirect pozzolanic reactivity testing methods, Buildings 13 (2023) 2789, https://doi.org/10.3390/buildings13112789.
[31] S. Donatello, M. Tyrer, C.R. Cheeseman, Comparison of test methods to assess pozzolanic activity, Cem. Concr. Compos. 32 (2010) 121–127, https://doi.org/10.1016/j.cemconcomp.2009.10.008.
[32] Hewlett, ed., Lea's Chemistry of Cement and Concrete: Hydration, Setting and Hardening of Portland Cement. Butterworth-Heinemann, [Lieu de publication non identifié]; 2003.